AIP | Applied Physics Letters

# Tunnel magnetoresistance properties and film structures of double MgO barrier magnetic tunnel junctions

H. D. Gan, S. Ikeda, W. Shiga, J. Hayakawa, K. Miura, H. Yamamoto, H. Hasegawa, F. Matsukura, T. Ohkubo, K. Hono, and H. Ohno

Citation: Applied Physics Letters **96**, 192507 (2010); doi: 10.1063/1.3429594
View online: http://dx.doi.org/10.1063/1.3429594
View Table of Contents: http://scitation.aip.org/content/aip/journal/apl/96/19?ver=pdfcov
Published by the AIP Publishing



# Tunnel magnetoresistance properties and film structures of double MgO barrier magnetic tunnel junctions

H. D. Gan,[1,2] S. Ikeda,[1,2,a)] W. Shiga,[2] J. Hayakawa,[3] K. Miura,[1,2,3] H. Yamamoto,[1,2,3] H. Hasegawa,[3] F. Matsukura,[1,2] T. Ohkubo,[4] K. Hono,[4] and H. Ohno[1,2,b)]
[1]*Center for Spintronics Integrated Systems, Tohoku University, 2-1-1 Katahira, Aoba-ku, Sendai 980-8577, Japan*
[2]*Laboratory for Nanoelectronics and Spintronics, Research Institute of Electrical Communication, Tohoku University, 2-1-1 Katahira, Aoba-ku, Sendai 980-8577, Japan*
[3]*Advanced Research Laboratory, Hitachi, Ltd., Kokubunji, Tokyo 185-8601, Japan*
[4]*National Institute for Materials Science, 1-2-1 Sengen, Tsukuba 305-0047, Japan*

(Received 27 January 2010; accepted 18 April 2010; published online 13 May 2010)

The authors fabricated double MgO barrier magnetic tunnel junctions (MTJs) with 3-nm-thick $Co_{40}Fe_{40}B_{20}$ free layer. When annealed at 350 °C, tunnel magnetoresistance (TMR) ratio at room temperature was 130%, much lower than that (297%) of single MgO barrier MTJs processed and annealed under the same condition. The middle CoFeB free layer sandwiched between the two MgO barriers was found to be mostly amorphous. Replacement of the $Co_{40}Fe_{40}B_{20}$ free layer by a highly oriented $Co_{50}Fe_{50}$ layer and a composite $Co_{50}Fe_{50}/Co_{40}Fe_{40}B_{20}$ layer led to the enhanced TMR ratios up to 165% and 212% at annealing temperature of 350 °C, respectively. © *2010 American Institute of Physics*. [doi:10.1063/1.3429594]

Progress of tunnel magnetoresistance (TMR) ratios for MgO-based magnetic tunneling junctions (MTJs) has contributed to the improved performance of spintronics devices such as magnetoresistive random access memories, nonvolatile logics, and hard disk drives based on MTJs.[1–8] In single MgO barrier MTJs (SMTJs), TMR ratios of up to 604% in pseudospin valve MTJs (Ref. 9) and 361% in exchange-biased MTJs[10,11] have been reported at room temperature (RT). Double barrier MTJ (DMTJ) structures are expected to be an effective means not only to improve the bias dependence of the TMR ratio, i.e., output voltage ($\Delta V = V \times (R_{AP} - R_P)/R_P = V \times$ TMR ratio, where $V$ is applied bias, and $R_P$ and $R_{AP}$ are resistances at parallel and antiparallel configurations, respectively),[12] but also to reduce the critical current density of spin torque transfer MTJs.[13] Furthermore, for DMTJs with ultrathin middle ferromagnetic layer (~1 nm), transport properties such as quantum confinement effect, Coulomb blockade and spin-dependent resonant tunneling have been predicted and observed.[14,15] Recently, a TMR ratio of 1056% at RT has been observed in DMTJs having a CoFeB layer at the continuous-discontinuous film border.[16] Although DMTJs with a thick middle free layer may offer a number of advantages, the reported TMR ratio[17–19] was much lower than those of SMTJs. The reason for the difference of the TMR properties between DMTJs and SMTJs has not yet been fully clarified. In this work, we studied the relationship between the TMR properties and film structures for DMTJs with 3-nm-thick $Co_{40}Fe_{40}B_{20}$ middle layer, and made an effort to enhance TMR ratio by optimizing the middle free layer structure.

Beginning from the substrate surface, the following layer sequence for the DMTJs were prepared on thermally oxidized Si wafers using ultrahigh vacuum rf-magnetron sputtering: Ta(5)/Ru(10)/Ta(5)/NiFe(3)/MnIr(8)/$Co_{50}Fe_{50}$ ×(2.5) / Ru(0.8) / $Co_{40}Fe_{40}B_{20}$(3) / MgO(2.1) / free-layer/ MgO(2.1) /$Co_{40}Fe_{40}B_{20}$(3) / Ru(0.8) / $Co_{50}Fe_{50}$(2.5) / MnIr ×(12)/Ta(5)/Ru(5) (in brackets the thickness of the single layers in nanometer). $Co_{40}Fe_{40}B_{20}$(3), $Co_{50}Fe_{50}$(3), or $Co_{50}Fe_{50}$(1)/$Co_{40}Fe_{40}B_{20}$(2) (in atomic percent) were used as the free layer. For comparison, SMTJs having a structure of Ta(5)/Ru(10)/Ta(5)/NiFe(3)/MnIr(8)/$Co_{50}Fe_{50}$(2.5)/ Ru(0.8)/$Co_{40}Fe_{40}B_{20}$(3)/MgO(2.1)/$Co_{40}Fe_{40}B_{20}$(3) /Ta(5)/ Ru(5) were also prepared. All MTJs were fabricated using photolithography and Ar ion milling with junction size of $0.8 \times 0.8 - 0.8 \times 5.6$ $\mu m^2$. And then the MTJs were annealed at annealing temperature ($T_a$) ranging from 270 to 350 °C in a vacuum of $10^{-6}$ Torr under a magnetic field of 0.4 T for 1 h. We measured the transport properties using a dc four-point probe method. The structural characterization was performed by high resolution transmission electron microscopy (HR-TEM) and energy filtering TEM (EF-TEM).

Figure 1(a) shows the $T_a$ dependence of TMR ratio at RT for the DMTJs and the SMTJs. The TMR ratios of the DMTJs and the SMTJs are almost the same at $T_a = 270$ °C,

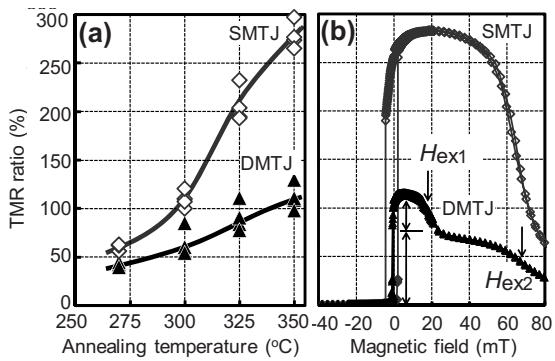


FIG. 1. (a) Annealing temperature ($T_a$) dependence of TMR ratio at RT of the DMTJs and SMTJs with 3-nm-thick $Co_{40}Fe_{40}B_{20}$ free layer. (b) Typical TMR loops of the DMTJ and the SMTJs.

a)Author to whom correspondence should be addressed. Electronic mail: sikeda@riec.tohoku.ac.jp.
b)Electronic mail: ohno@riec.tohoku.ac.jp.

 

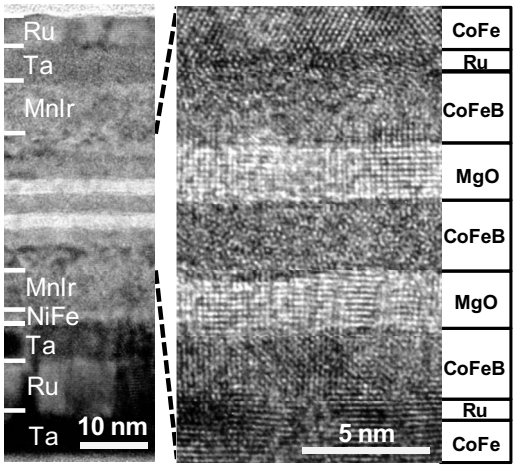


FIG. 2. Cross-sectional HRTEM images of the DMTJ with $Co_{40}Fe_{40}B_{20}$ free layer annealed at 350 °C.

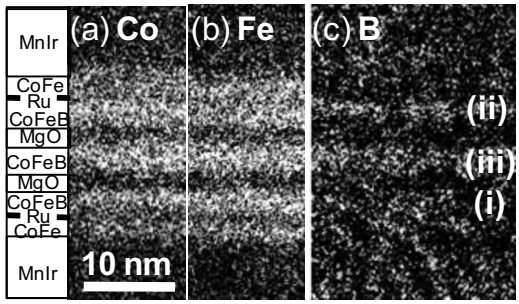


FIG. 3. Energy filtered TEM (EF-TEM) images of (a) Co, (b) Fe, and (c) B elements in the DMTJ with $Co_{40}Fe_{40}B_{20}$ free layer annealed at 350 °C. In the elemental maps, the higher intensity (i.e., brighter region) corresponds to the higher concentration of the constituent elements. Three characteristics of B element can be seen as follows: (i) B concentration in the bottom reference layer is very low, (ii) B in the top layer has segregated at the top reference layer/Ru interface, and (iii) B in the middle CoFeB free layer is largely uniformly distributed.

and then monotonically increase with $T_a$. At $T_a$=350 °C, the TMR ratio of the SMTJs reaches 297%, whereas the TMR ratio of the DMTJs is only 130%, which is similar to or slightly higher than those of DMTJs with similar free layer thickness reported by other groups.[16–20] Figure 1(b) shows representative TMR loops of the DMTJ and the SMTJ annealed at $T_a$=350 °C. The TMR loop of the DMTJ has three steps corresponding to the magnetization reversal of a free layer and two reference layers. Coercivity of the free layer in DMTJ is 0.5 mT, which is lower than that (3.3 mT) of SMTJ. The exchange bias fields of the top and bottom reference layers are about $H_{ex1}\sim 17$ mT and $H_{ex2}\sim 68$ mT, respectively. As shown by the arrows in Fig. 1(b), the contribution to the TMR properties of the top junction is weaker than that of bottom junction.

To understand the reason for the low TMR ratio of the DMTJs, the film structures were investigated by HRTEM. Figure 2 shows the cross-sectional HRTEM images of the DMTJ annealed at $T_a$=350 °C. The two MgO barriers have highly (001)-oriented texture. The top and the bottom CoFeB reference layers are crystallized with the (001)-oriented texture, whose lattice fringes are completely coherent with those of the MgO barriers. The degree of crystallization in the top CoFeB reference layer is slightly less than the bottom one, which may be a factor for the low TMR of the top junction. On the other hand, the middle CoFeB free layer sandwiched between the two MgO barriers is hardly crystallized and remains mostly amorphous, which is believed to be responsible for the low TMR ratio of the DMTJs.

The suppression of the crystallization of the middle CoFeB layer in the DMTJs is likely related to the way B diffuses: B cannot be dissolved in CoFe, so B is rejected on crystallization of CoFeB amorphous phase.[21] In the SMTJs, the B rejected from the CoFe phase that was heterogeneously nucleated from the MgO/CoFeB interface diffuses into the adjacent metallic layers during annealing.[22–25] In the DMTJs, B diffusion in the middle CoFeB free layer is possibly suppressed by the top and bottom MgO barriers. Since the partitioning of B to the residual amorphous phase is required for the nucleation of the primary CoFe phase, the crystallization would be suppressed without B rejection to the adjacent metallic layers. To investigate the distribution of B in the DMTJs, EF-TEM mapping was employed. Figure 3 shows the energy filtered images of Co, Fe, and B taken from the respective ionization major edges for the DMTJ with the CoFeB free layer annealed at 350 °C. The high intensity (i.e., bright region) in the elemental maps corresponds to high concentration of the constituent elements. The Co and Fe maps [see Figs. 3(a) and 3(b)] suggest their uniform distribution in the CoFe pinned layers and the CoFe(B) free and reference layers. In the B map [see Fig. 3(c)], three following characteristics can be seen: (i) B concentration in the bottom reference layer is very low, if there is any, (ii) B in the top layer has segregated at the top reference layer/Ru interface, and (iii) B in the middle CoFeB free layer is largely uniformly distributed, which suggests that B does not diffuse out of the CoFeB layer, at least not beyond the experimental resolution, into the bottom and top MgO barriers. The different distributions of B correspond with the degree of crystallization of the three CoFeB layers, that is, the bottom reference layer is crystallized completely, the top reference layer has a reduced degree of crystallization compared to the bottom one, and the middle free layer has hardly crystallized. These structural features are consistent with the low TMR ratio for the DMTJs, reduced TMR of the top junction, and the low coercivity of the middle free layer of DMTJs. Crystallization of the middle CoFeB free layer is related not only to the B diffusion but probably also to the interface energy resulting from the lattice mismatch at the CoFeB/MgO interfaces.[26] The interface energy acting on free layer in the DMTJs is expected to be higher than that of the free layer in the SMTJs because of the two CoFeB/MgO interfaces. High interface energy reduces the nucleation rate and thus can result in the suppression of partial crystallization in the middle CoFeB layer.[27]

The above results suggest that higher TMR ratio may be obtained by using crystalline bcc(001)-CoFe as the middle free layer. In our previous studies, the growth of (001)-oriented $Co_{50}Fe_{50}$ on MgO and (001)-oriented MgO on (001) $Co_{50}Fe_{50}$ have been observed.[28,29] We thus examined the influence of $Co_{50}Fe_{50}$ free layer on TMR ratio for DMTJs. As can be seen in Fig. 4(a), by replacing the middle layer with a $Co_{50}Fe_{50}$ layer, the TMR ratio was enhanced and reached 165% at $T_a$=350 °C. Moreover, by the use of a composite $Co_{50}Fe_{50}/Co_{40}Fe_{40}B_{20}$ layer, the TMR ratio further increased to 212% at $T_a$=350 °C. The enhancement of the TMR ratio of the DMTJ with the composite $Co_{50}Fe_{50}/Co_{40}Fe_{40}B_{20}$ free layer can be attributed to (001)-oriented $Co_{50}Fe_{50}$ layer on

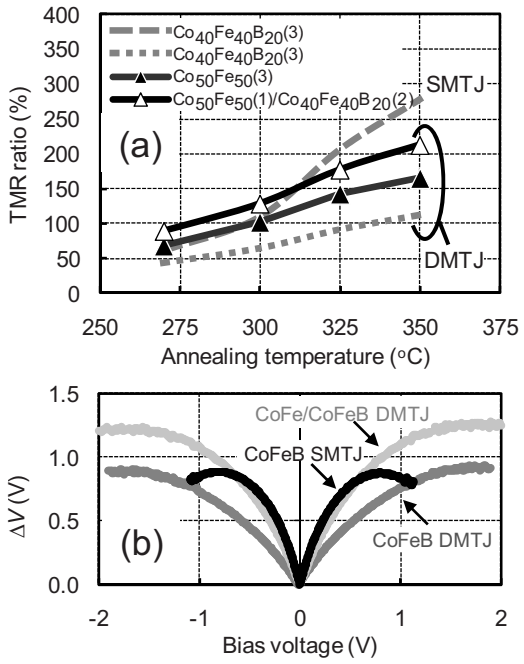


FIG. 4. (a) Annealing temperature ($T_a$) dependence of the TMR ratio and (b) the bias voltage dependence of the output voltage ($\Delta V$) for the DMTJs with different free layer and the SMTJs for comparison.

bottom-MgO barrier as well as the formation of highly (001)-oriented top MgO-barrier on the amorphous $Co_{40}Fe_{40}B_{20}$ layer. Figure 4(b) shows the applied bias dependence of output voltage $\Delta V$ of the SMTJ and the DMTJs with $Co_{40}Fe_{40}B_{20}$ and $Co_{50}Fe_{50}/Co_{40}Fe_{40}B_{20}$ free layers. By the use of DMTJ structure, we confirmed the improvement of bias dependence of $\Delta V$, i.e., TMR properties. The highest $\Delta V$ of 0.93 V and 1.27 V for the DMTJs with $Co_{40}Fe_{40}B_{20}$ and $Co_{50}Fe_{50}/Co_{40}Fe_{40}B_{20}$ composite free layers are obtained, respectively.

In summary, we studied the TMR ratio of DMTJs with 3-nm-thick CoFe(B) free layer. The TMR ratio of 130% in the DMTJs with $Co_{40}Fe_{40}B_{20}$ annealed at $T_a$=350 °C was lower than that (297%) of SMTJs. HRTEM showed that the middle CoFeB free layer sandwiched between the two MgO barriers remained mostly amorphous, which we attributed to the suppression of B diffusion. By applying the crystalline $Co_{50}Fe_{50}$ and composite $Co_{50}Fe_{50}/Co_{40}Fe_{40}B_{20}$ free layers, the TMR ratio was enhanced to 165% and 212% at $T_a$ =350 °C, and the output voltage showed 0.93 V and 1.27 V, respectively.

This work was partially supported by the "High-Performance Low-Power Consumption Spin Devices and Storage Systems" program under Research and Development for Next-Generation Information Technology of MEXT, by the Japan Society for the Promotion of Science (JSPS) through its "Funding Program for World-Leading Innovative R&D on Science and Technology (FIRST Program)", and by a Grant-in-Aid for Scientific Research in Priority Area "Creation and Control of Spin Current," by the World Premier Research Center Initiative (WPI Initative) on Materials Nanoarchitectronics of MEXT. The authors wish to thank Y. Ohno and K. Ohtani for discussion and I. Morita and T. Hirata for their valuable discussions and technical support in MTJ fabrication.

[1]W. H. Butler, X.-G. Zhang, T. C. Schulthess, and J. M. MacLaren, Phys. Rev. B **63**, 054416 (2001).
[2]J. Mathon and A. Umersky, Phys. Rev. B **63**, 220403 (2001).
[3]S. Yuasa, A. Fukushima, T. Nagahama, K. Ando, and Y. Suzuki, Nature Mater. **3**, 868 (2004).
[4]S. S. Parkin, C. Kaiser, A. Panchula, P. M. Rice, B. Hughes, M. Samant, and S. H. Yang, Nature Mater. **3**, 862 (2004).
[5]D. D. Djayaprawira, K. Tsunekawa, M. Nagai, H. Maehara, S. Yamagata, N. Watanabe, S. Yuasa, Y. Suzuki, and K. Ando, Appl. Phys. Lett. **86**, 092502 (2005).
[6]J. Hayakawa, S. Ikeda, F. Matsukura, H. Takahashi, and H. Ohno, Jpn. J. Appl. Phys., Part 2 **44**, L587 (2005).
[7]T. Kawahara, R. Takemura, K. Miura, J. Hayakawa, S. Ikeda, Y. M. Lee, R. Sasaki, Y. Goto, K. Ito, T. Meguro, F. Matsukura, H. Takahashi, H. Matsuoka, and H. Ohno, IEEE J. Solid-state Circuits **43**, 109 (2008).
[8]S. Matsunaga, J. Hayakawa, S. Ikeda, K. Miura, H. Hasegawa, T. Endoh, H. Ohno, and T. Hanyu, Appl. Phys. Express **1**, 091301 (2008).
[9]S. Ikeda, J. Hayakawa, Y. Ashizawa, Y. M. Lee, K. Miura, H. Hasegawa, M. Tsunoda, F. Matsukura, and H. Ohno, Appl. Phys. Lett. **93**, 082508 (2008).
[10]Y. M. Lee, J. Hayakawa, S. Ikeda, F. Matsukura, and H. Ohno, Appl. Phys. Lett. **89**, 042506 (2006).
[11]J. Hayakawa, Y. M. Lee, S. Ikeda, F. Matsukura, and H. Ohno, Appl. Phys. Lett. **89**, 232510 (2006).
[12]K. Inomata, Y. Saito, K. Nakajima, and M. Sagoi, J. Appl. Phys. **87**, 6064 (2000).
[13]Z. Diao, A. Panchula, Y. Ding, M. Pakala, S. Wang, Z. Li, D. Apalkov, H. Nagai, A. Driskill-Smith, L.-C. Wang, E. Chen, and Y. Huai, Appl. Phys. Lett. **90**, 132508 (2007).
[14]T. Nozaki, N. Tezuka, and K. Inomata, Phys. Rev. Lett. **96**, 027208 (2006).
[15]X. Zhang, B. Li, G. Sun, and F. Pu, Phys. Rev. B **56**, 5484 (1997).
[16]L. Jiang, H. Naganuma, M. Oogane, and Y. Ando, Appl. Phys. Express **2**, 083002 (2009).
[17]T. Nozaki, A. Hirohata, N. Tezuka, S. Sugimoto, and K. Inomata, Appl. Phys. Lett. **86**, 082501 (2005).
[18]G. Feng, S. van Dijken, and J. M. D. Coey, Appl. Phys. Lett. **89**, 162501 (2006).
[19]J. M. Almeida, P. Wisniowski, and P. P. Freitas, J. Appl. Phys. **103**, 07E922 (2008).
[20]G. Feng, S. van Dijken, J. F. Feng, J. M. D. Coey, T. Leo, and D. J. Smith, J. Appl. Phys. **105**, 033916 (2009).
[21]C. Y. You, T. Ohkubo, Y. K. Takahashi, and K. Hono, J. Appl. Phys. **104**, 033517 (2008).
[22]S. Yuasa, Y. Suzuki, T. Katayama, and K. Ando, Appl. Phys. Lett. **87**, 242503 (2005).
[23]T. Miyajima, T. Ibusuki, S. Umehara, M. Sato, S. Eguchi, M. Tsukada, and Y. Kataoka, Appl. Phys. Lett. **94**, 122501 (2009).
[24]T. Ibusuki, T. Miyajima, S. Umehara, S. Eguchi, and M. Sato, Appl. Phys. Lett. **94**, 062509 (2009).
[25]S. V. Karthik, Y. K. Takahashi, T. Ohkubo, K. Hono, S. Ikeda, and H. Ohno, J. Appl. Phys. **106**, 023920 (2009).
[26]K. Tsunekawa, Y. S. Choi, Y. Nagamine, D. D. Djayaprawira, T. Takeuchi, and Y. Kitamoto, Jpn. J. Appl. Phys., Part 2 **45**, L1152 (2006).
[27]Y. M. Lee, J. Hayakawa, S. Ikeda, F. Matsukura, and H. Ohno, Appl. Phys. Lett. **90**, 212507 (2007).
[28]S. Ikeda, J. Hayakawa, Y. M. Lee, T. Tanikawa, F. Matsukura, and H. Ohno, J. Appl. Phys. **99**, 08A907 (2006).
[29]S. Ikeda, J. Hayakawa, Y. M. Lee, F. Matsukura, and H. Ohno, J. Magn. Magn. Mater. **310**, 1937 (2007).